

Study of Two-Phase Flow Behavior around Chute Aerator Using OpenFOAM

Hamzeh Ebrahimnezhadian^a, Mohammad Manafpour^{a,*}

^aDepartment of Civil Engineering, Urmia University, 11Km Sero Road, Urmia, 5756151818, Iran

Corresponding author: *m.manafpour@urmia.ac.ir

Abstract—Aeration devices are installed on chute spillways to prevent cavitation damage in high-velocity flows. Large quantities of air-entrained characterize bottom aerators along with the jet interfaces and a strong de-aeration process near the impact of the water jet with the spillway bottom. Appropriate prediction of the air entrainment process, flow characteristics, and two-phase flow pattern at the aerator would contribute to reliable spillway operation. The mathematical formulation of two-phase flow at an aerator remains a challenging issue for spillway design due to its complexities. In the present study, 2D numerical simulations are performed to predict the distribution of air concentrations, flow velocity, turbulent intensity, and water surface profile along the chute aerator using open-source OpenFOAM software and RNG k- ϵ turbulent model. The correlation coefficients obtained between the numerical and experimental results indicate that a proper agreement exists between the relative cavity length and velocity profile results. The research results show that the turbulent intensity of flow passing over the aerator ramp is significantly increases. It means that the ramp acts as a turbulent generator on the spillway chute. The maximum value of turbulence intensity occurs at the 6-8% of flow depth(h) from the tip of the ramp, and it is raised as the Froude number increases. It is concluded that the intake air flow rate and air-entrainment coefficient (β) are linearly increased concerning the Froude number.

Keywords— Aerator ramp; air entrainment; cavity length; RNG k- ϵ turbulence model; OpenFOAM.

Manuscript received 25 Oct. 2019; revised 5 Dec. 2020; accepted 10 Feb. 2021. Date of publication 31 Aug. 2021. IJASEIT is licensed under a Creative Commons Attribution-Share Alike 4.0 International License.



I. INTRODUCTION

Spillways and chutes operating under high-velocity flows are at risk of the cavitation phenomenon, which causes major damages or endangers the dam stability. Therefore, in engineering designs, it is necessary to protecting spillways against cavitation damage [1]. Control of cavity bubbles collapse near the solid boundary and use of cavitation-resistant materials are some approaches for preventing cavitation damage [2]. Aeration is the most efficient and economical method for preventing cavitation in high-speed flows over chute spillways [3], [4]. With 8% air near the concrete surface, damage of cavitation attack is completely prevented [5]. Aeration can occur in both natural and induced forms. Air entrained through flow-free surface results in a “white water” region at the free surface and is not sufficient to reduce the damage risk of cavitation phenomenon on solid boundary [2]. Free-surface aeration occurs whenever the thickness of the turbulent boundary layer reaches the depth of flow. Free-surface aeration alone is not sufficient to avoid or reduce the possibility of

cavitation damage [6]. Injecting air into the flow is one of the best and most economical ways to protect the surface of the spillway against cavitation damage. Therefore, with regard to the danger of cavitation attack, induced aeration of flow is recommended [7]. The flow is separated from the spillway surface by a geometrical device, which forms a nappe and leads to aerated flow, as shown in Figure 1. These devices, which are used to inject air into the flow, are called aerators and are usually installed on the spillway floor and also on the side walls (Figure 2) [2], [8].

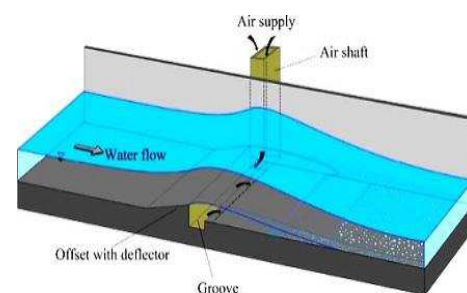


Fig. 1 aerator configuration [12]



Fig. 2 Flow aeration systems [12]

A small deflection on a chute bed (e.g., ramp) tends to separate the flow away from the chute surface. In the cavity formed below the nappe, a local sub pressure (ΔP) is produced by which air is dragged into the flow (Q_{air} inlet). The main flow regions in the vicinity of a bottom aerator are the approach flow region, the transition region, the aeration region, the reattaching region, and the downstream flow region (Figure 3) [9].

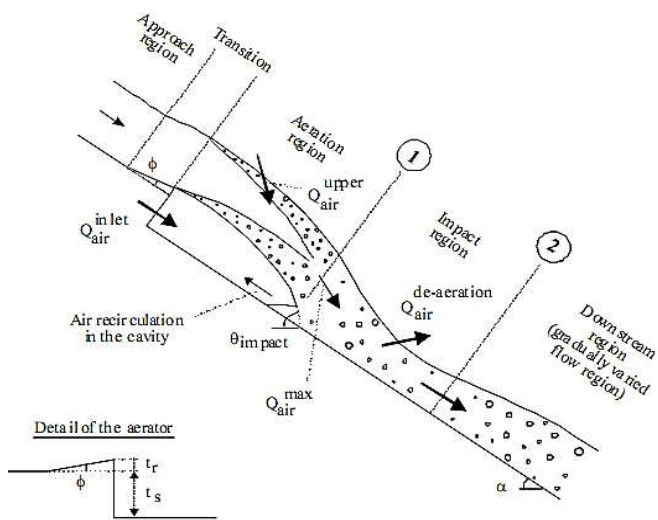


Fig. 3 Flow regions above a ramp aerator

A review of Flow behavior on an aerator ramp (Figure 3) shows the complex interaction between turbulent flow structure, the phenomenon of cavitation, the jet development in the atmosphere, the air entering into the jet, as well as the propagation of bubbles in the flow downstream of the ramp. Air is entrained along the lower and upper surface of the nappe. The more downward surface entrainment introduces air bubbles near the bed of the spillway for some distance downstream [10]. Proper recognition of the two-phase flow pattern in free surface flow spillways is among the topics studied by some researchers. However, there is a necessity for further laboratory and numerical studies in this field due to the flow complexity.

Researchers in the field of hydraulics have studied aeration tools such as ramps for years, both in the laboratory and field observations [11]. Since aerators' field observations are associated with limitations, laboratory studies have been used by researchers as a major research tool in this field for many years. Despite the prevalence of laboratory research, its cost and timeliness have always been a major problem. Researchers have done a lot of research to achieve empirical equations to estimate the characteristics of aerated flow.

However, the equations are generally not practical in design [12], [13]. Kramer and Hager [14] investigated the flow characteristics such as velocity, air demand, and air bubble size distributions experimentally. They found that the bubble rise velocity in chute flows on the Froude number.

Computational fluid dynamics is used as an essential complement to laboratory studies in two-phase flow modeling. CFD helps us to investigate the aerated flow field numerically in detail. Some researchers who employed the VOF and Mixture models to study an aerated flow found that the Mixture model is more suitable for simulating this type of flow, especially with high air concentration [15]. Zhang [16] carried out three-dimensional modeling using the Mixture approach. He evaluated aerated flow characteristics such as air bubble diameter; he found that smaller air bubble diameter leads to better agreement with experimental results. Ruidi *et al.* [17] examined the air concentration and bubble characteristics downstream of the chute aerator laboratory. Based on their research results, they presented a formula for the maximum frequency of air bubbles. Teng *et al.* [18] created a 3D numerical model using the VOF approach for flow over MOFORSÉN dam aerator and compared the results with field measurement. The results show good agreement between the flow field measurement and numerical models. Lian *et al.* [19] investigated air entrainment and air demand in the Spillway Tunnel using numerical models, laboratory experiments, and field measurement. They found a remarkable difference between the results from the prototype and laboratory experiments, which indicates the scale effect in the physical model. Yang *et al.* [20]-[22] conducted numerical research and used fluent software to investigate the effect of flow aeration in wide spillway aerators. The results showed that wide spillway aerators play a significant role in flow aeration, and this effect has a higher percentage difference near the wall and chute center zones than normal spillway aerators. By conducting a series of experiments, Ruidi *et al.* [23] examined the characteristics of the flow around the aerator, including the amount of air entering the flow. The results showed that air entrainment is directly related to the Froude number. Sarvar *et al.* [24] evaluated orifice spillway aerators' function with different slopes using a numerical and experimental model. They developed an empirical equation based on results that will be appropriate for the orifice spillway aerators with a slope from 26° to 32° . Yang *et al.* [25] studied two-phase flows in a large chute aerator numerically. The result showed that for characteristics such as cavity length and air ratio, the better adaptation of laboratory and numerical results occurs when smaller air bubble diameters are used. Cihan Aydın [26], [27] performed various laboratory tests for different Froude number and ramp heights to evaluate spillway aerators' performance. This study's results led to experimental relationships for estimating the air intake coefficient, which showed high compliance with laboratory results.

This study aims to investigate numerically the characteristics of flow passing an aerator ramp installed on the chute bed. Especial attention are given to determine the distribution of flow velocity, air concentration, and turbulent intensity along the chute. Also, the effect of the flow Froude

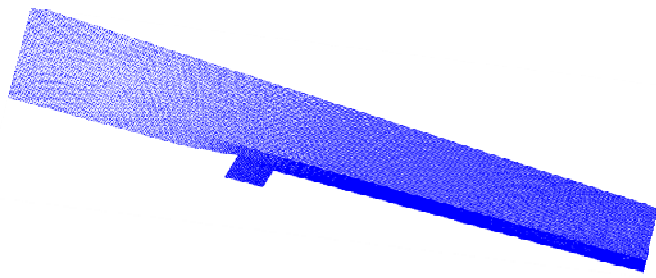


Fig. 5 Flowfield meshing and boundary condition

In this research, the following boundary conditions are used for the numerical model; 1- water inlet: mass flow rate 2- air inlet: mass flow rate 3- outlet: pressure outlet 4- channel body such as the floor, ramp and side walls: wall, 5- channel roof: atmosphere.

III. RESULT AND DISCUSSION

The numerical model's performance is verified using the experimental results of cavity length formed immediately downstream of the ramp, and the mean flow velocity. In the next step, the flow characteristics along the chutes such as velocity, air concentration, turbulent intensity and water surface profile for some runs are numerically extracted and discussed where a broad understanding of flow behaviour around the aerator ramp has been achieved.

A. Verification of Numerical Model

1) *Cavity Length (L_c):* The deflector separates water flow passing over the aerator ramp from the chute bottom, and a cavity is formed immediately downstream of the ramp. As a result, airflow is forcefully drawn into the cavity. The cavity length, marked as L_c (m), is the distance from the aerator ramp to the point where the jet hits the floor of the chute (reattachment point R) (Figure 6). To delineation the air-entrainment capacity of an aerator, coefficient (β) is defined as the ratio of airflow discharge (Q_a , m^3/s) to water flow discharge (Q_w , m^3/s).

Figure 7 demonstrates the comparison of the cavity lengths (L_c) gained from the numerical and laboratory models for different runs. For all runs, the cavity lengths are estimated by the two-dimensional numerical model more than the laboratory model. The difference percentages calculated for the two models' cavity lengths are less than 8%, confirming that the simulation carried out by the numerical model is satisfactory.

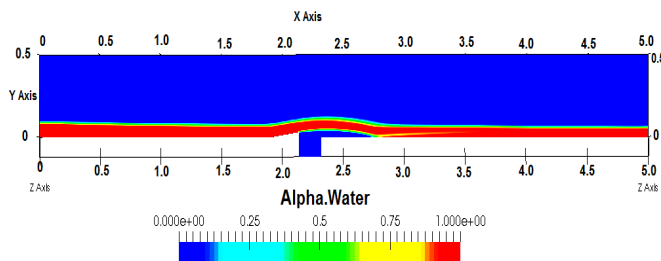


Fig. 6 Flow field of the numerical model

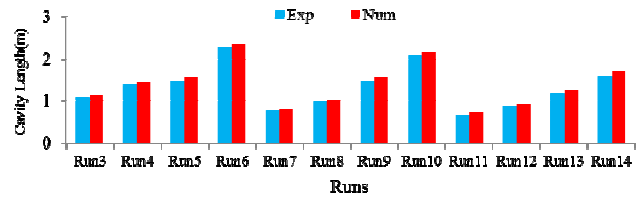


Fig. 7 Comparison of the cavity lengths obtained from numerical and laboratory models for various runs

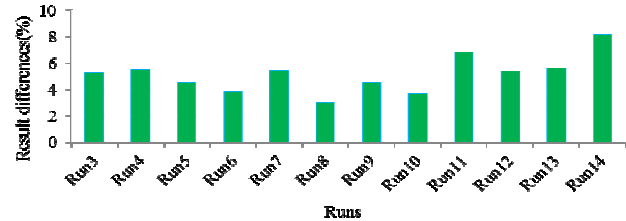


Fig. 8 Differences between the numerical and laboratory results of the cavity lengths for various runs

2) *Mean velocity:* The mean velocity distribution profiles obtained from the numerical and laboratory models in the flow direction is displayed in Figure 8 on the ramp tip (Section S_3 seen in Figure 3) for runs 3 and 5 ($t_r=4cm$, $\theta=10^\circ$). The conformity of numerical and experimental results implies that the numerical model appropriately simulates the aerator ramp's flow velocity field. As shown in Fig. 9, the flow velocity gradually increased from the bed bottom to reaching a threshold value.

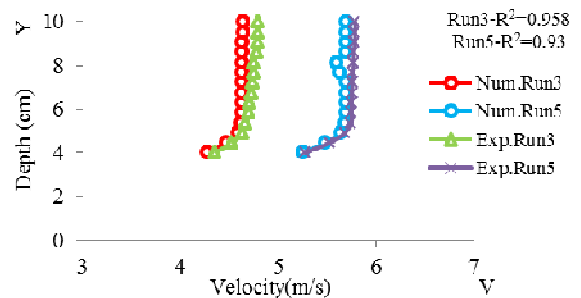


Fig. 9 Comparison of the flow velocity profiles between numerical and laboratory models at Section S_3 for runs 3 and 5

B. Variation of Flow Characteristics around the Aerator Ramp

In order to better understanding the flow field in the vicinity of the aerator ramp, variations of flow characteristics such as velocity, air concentration, turbulent intensity, and water surface are investigated. Profiles of these characteristics obtained from the numerical model are presented in various sections along the chute. Coordinate of these 12 sections is displayed in Table II as well as Figure 10. Furthermore, the effect of the Froude number of approaching flow is studied on the turbulence intensity and aeration coefficient of flow passing the aerator ramp.

Section	S ₁	S ₂	S ₃	S ₄	S _{4C}	S ₅	S ₆
X(m)	1.54	1.84	2.04	2.20	2.23	2.32	2.44
Section	S ₇	S ₈	S ₉	S ₁₀	S ₁₁	S ₁₂	
X(m)	2.74	3.04	3.5	4.0	4.5	4.8	

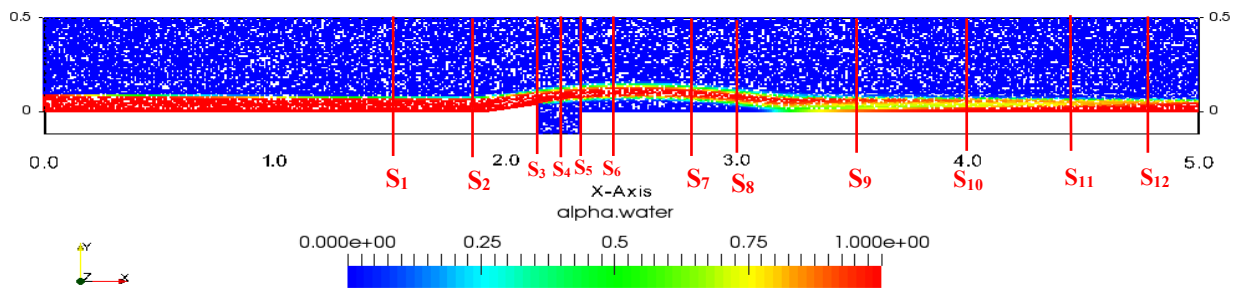


Fig. 10 Location of the sections along the chute

1) *Velocity Profiles*: Velocity Profiles are presented in Figure 10 at 12 sections along the chute for Run8 ($t_r=4\text{cm}$, $\theta=10^\circ$, $\varphi=14.5^\circ$) where θ and φ are angles of the ramp and chute bed, respectively. As shown in Figure 11, in all profiles (before the ramp, over and after the ramp), the flow velocity gradually increased from the minimum value on the floor to a threshold value. Velocity profiles at upstream of the ramp (S_1 , S_2), on the tip of the ramp (S_3) and Shortly

thereafter (S_4 , S_{4c}), on cavity region (S_5 , S_6 , S_7), near reattachment point (S_8), and downstream region of reattachment point (S_9 , S_{10} , S_{11} , S_{12}) have a variety of forms depending on the hydraulic and geometrical conditions.

As seen (Figure 11) from profile S_8 near the jet collision region, the flow velocity near the floor is significantly reduced compared to the other profiles due to the jet collision with the floor.

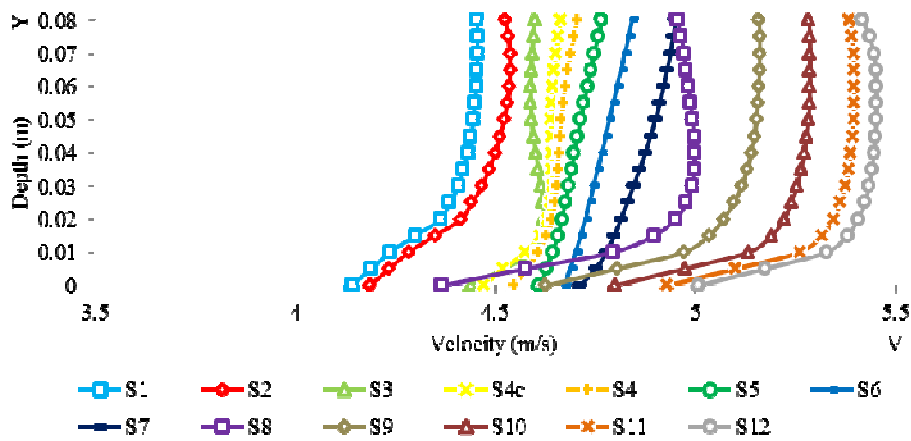


Fig. 11 Velocity distribution profiles at different sections around the chute aerator

2) *Air Concentration Profiles*: In this simulation, the flow field is aerated by two mechanisms: 1) natural entrainment from upper nappe of jet; 2) from lower nappe of the jet in which aerated top boundary of the cavity where a strong turbulent happens. The percentage of aeration from the lower surface of the jet at the reattachment point is considerable due to the higher level of turbulence. Figure 12 shows the C distribution as a function of the relative depth of flow (Y/Y_{C90}), in which Y is water depth, and Y_{C90} is water depth where $C=90\%$ at different sections.

As seen from Figure 12, at section S_1 , located upstream of the ramp aerator, there is no air in the lower layer of water flow close to the chute bed. Air is gradually entrained into the flow-through free surface. S_3 to S_7 placed in the cavity

zone downstream of the ramp, C , which is maximum inside the cavity, is gradually reduced by moving upward in the water body until half of the water depth where air concentration is reached to a minimum value. After that C is progressively increased to a maximum amount on the free surface of the water. Downstream of the cavity zone, the de-aeration process in flow direction causes air bubbles to escape through the free surface; thus, uniform flow is formed with a steady distribution of C , as seen in section S_{11} of Figure 12. The variation pattern of C obtained here in the vicinity of the aerator ramp adapts similar research results found in the literature [13]–[15].

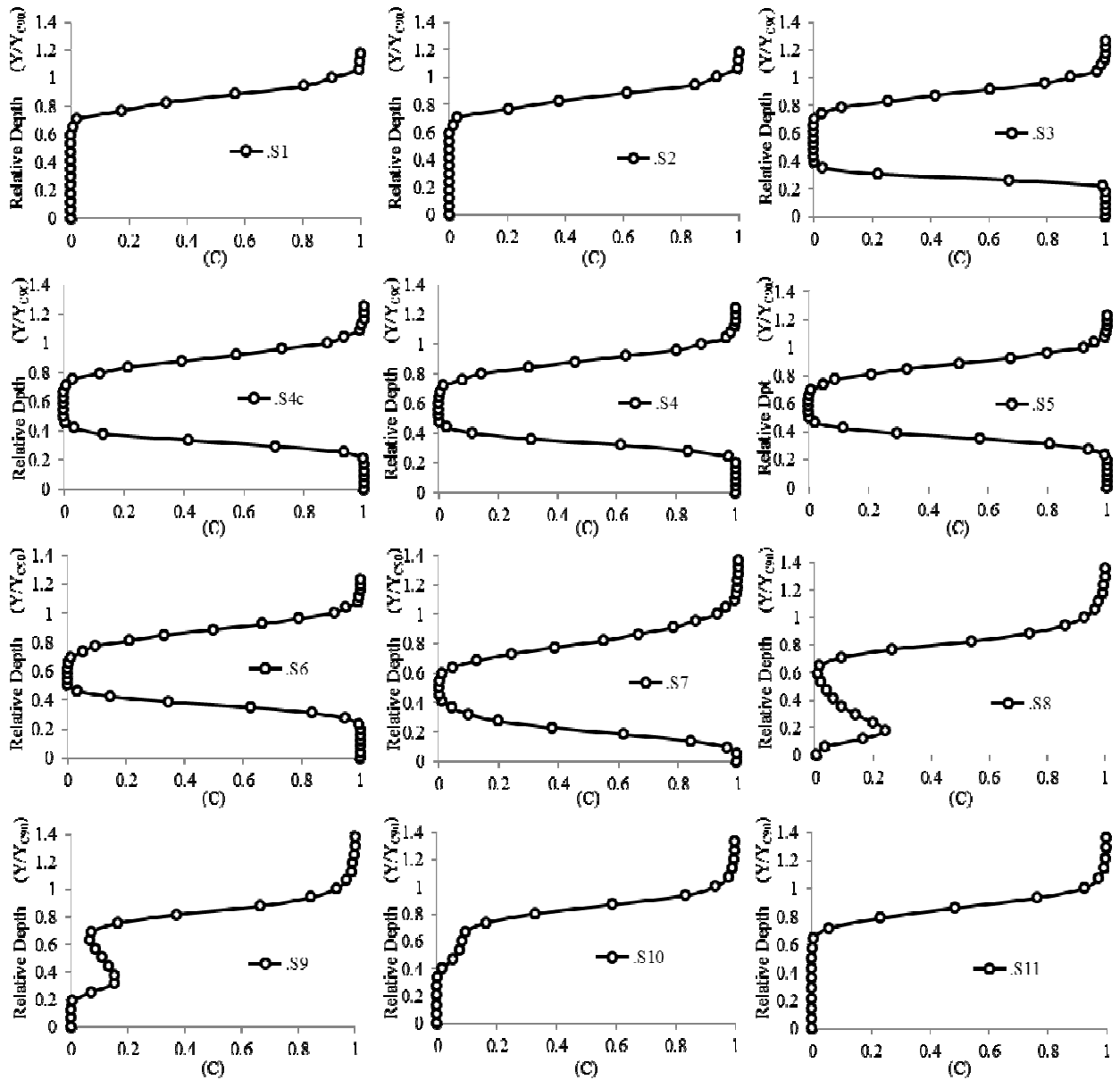


Fig. 12 Air concentration profiles at different sections around the chute aerator

3) *Water Surface Profile:* The water surface profile along the chute for Run 8 is presented in Figure 13. It is seen that water depth which is 9cm at the chute inlet, decreases slowly till the position of the ramp. It increases slightly over

the ramp and fluctuates at the reattachment zone. Thereafter it reduces progressively till the end of the chute. On the contrary, the flow velocity increases slowly along the chute.

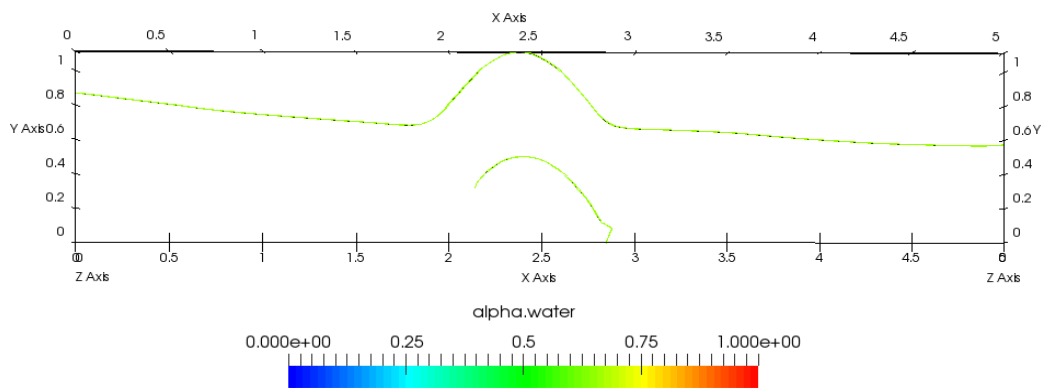


Fig. 13 Water surface Profile around the chute aerator

4) *Turbulent Intensity Profiles:* Figure 14 shows the distribution of Turbulent Intensity ($Tu = u'/U$) at various vertical sections around the aerator ramp. Where u' and U are velocity fluctuation and mean velocity, respectively. Also, Z is the height from the bottom of the flow body, and h is the water depth. As seen from Figure 14, the turbulent intensity along the aerator ramp is increased from small amounts at the beginning of the ramp (Section S2) to maximum values at the end of the ramp (Section S3); therefore ramp acts as a turbulent generator. After the ramp, the turbulent intensity gradually decreased along the chute.

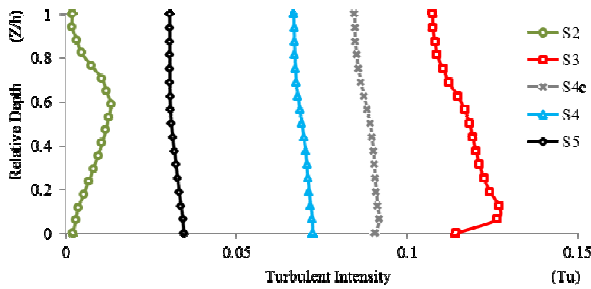


Fig. 14 Turbulent intensity profiles at different sections around the chute aerator

5) *Flow Turbulent Intensity versus Froude Number:* To investigate the variation of the turbulent intensity parameter of flow against Froude number, simulations are carried out for flows of 5 different Froude numbers ranging from 5.5 to 8.5. The profiles of the turbulent intensity distribution are demonstrated at section S_3 positioned on the aerator tip for various Froude numbers (Figure 15).

The results indicate that the rate of turbulent intensity is relatively increased when the Froude number grows. For a constant Froude number, the turbulent intensity gradually increases from the ramp tip up to a maximum value at the level of 6-8% of flow depth and thereafter, it reduces to a minimum amount close to the water-free surface, as seen from Figure (15a, b).

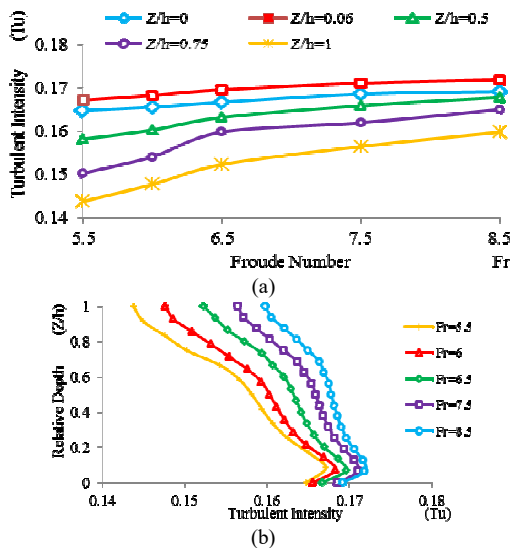


Fig. 15 a) Tu against Fr for various Z/h b) Tu profiles at Section 3 for various Fr

6) *Aeration Coefficient (β) versus Froude Number:* the air-entrainment capacity of an aerator that is expressed as an aeration coefficient (β) is defined as the ratio of air discharge (Q_{air} , m^3/s) to water flow discharge (Q_w , m^3/s). In order to calculate accurately the amount of air entering the flow through the aerator system mounted on the chute bed, the airflow is measured at the sections before ramp (S_2) and after the reattachment point (S_9). The differences between these sections' obtained values indicate the exact amount of air entering by the aerator into the flow. Figure 16 shows how the air discharge (Q_{air} , m^3/s) and aeration coefficient (β) change by increasing the Froude number from 5.5 to 8.5. These Froude numbers correspond to 30, 50, 70, 90, 110 and 130 lit/s water discharge (Q_w). The results show that the air-entrainment coefficient (β) increases linearly with the increase of the Froude number.

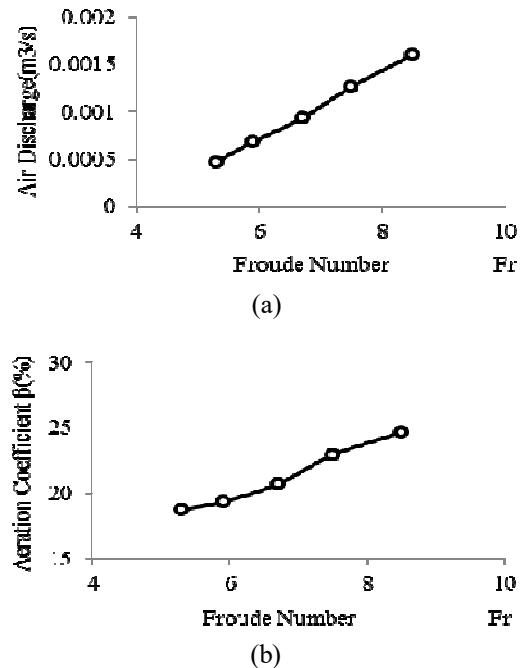


Fig. 16 Variation of a) Air discharge (Q_{air}) b) Aeration coefficient (β) against Froude number

IV. CONCLUSION

The results of this numerical investigation on the flow field around the chute aerator using OpenFOAM open-source software can be summarized as follows: Verification of results indicates a proper agreement between numerical and experimental results so that the difference between the numerical and laboratory results for the cavity length is, on average, 5% for all performances. R-squared results are 0.958 and 0.93 for the velocity result of RUN 3 and 5, respectively. Also, the modeling capability of the multiPhaseEulerFoam solver is justified by simulating the air-water flow around the chute aerator. Velocity increased gradually from the chute bed and reached maximum value on the near water surface. As the Froude number increases, the turbulence intensity profiles at the tip of the ramp show an increasing trend; thus, the ramp acts as a turbulent generator. The maximum value of turbulence intensity occurs at 6-8% of flow depth (h) on the tip of the ramp. As

the Froude number increases, both air flow discharge (Q_a) and aeration coefficient (β) increase linearly.

NOMENCLATURE

h	water depth	m
Q_{air}	air discharge	m^3s^{-1}
Q_w	water discharge	m^3s^{-1}
Y_{C90}	water depth where $C=90\%$	m
T_u	turbulent intensity	
L_C	cavity length	m
u'	velocity fluctuation	ms^{-2}
U	mean velocity	ms^{-2}
Z	height from the bottom of water body	m
Greek letters		
θ	aerator ramp angle	deg
β	aeration coefficient	
ρ	water density	$kg.m^{-3}$
φ	chute angle	deg

REFERENCES

- [1] H. Falvey, "Cavitation in Chutes and Spillways" Engineering Monograph 42, United States Department of the Interior, Bureau of Reclamation, Denver, Colo, USA. 1990.
- [2] J. A. Kells, and C. D. Smith, "Reduction of cavitation on spillways by induced air entrainment" *Canadian Journal of Civil Engineering*, Vol 18, pp. 358–377, 1991.
- [3] N. L. Pinto, "Prototype aerator measurements" IAHR Hydraulic Structures Design Manual No. 4, Ed. I.R, 1991.
- [4] W. Wei, J. Deng, and Z. Faxing "Development of self-aeration process for supercritical chute flows" *International Journal of Multiphase Flow*, Vol 79, pp. 172–180, 2016.
- [5] A. J. Peterka, "The effect of entrained air on cavitation pitting" *Joint Meeting Paper, IAHR/ASCE*, Minneapolis, Minnesota, pp. 507-518, Aug. 1953.
- [6] J. M. Zhang, J. G. Chen, and W. L. Xu, "Three-dimensional numerical simulation of aerated flows downstream sudden fall aerator expansion in a tunnel" *Journal of Hydrodynamics*, Vol 23(1), pp. 71–80, 2011.
- [7] R.W.P. May, P. M. Brown, and I. R. Willoughby, "Physical and numerical modeling of aerators for dam spillways" *Hydraulics Research Report*, No. SR 278, Wallingford, U.K. 1991.
- [8] D. Vischer, , P. Volkart, and A. Sigenthaler, "Hydraulic modelling of air slots in open chute spillways" *International Conference on the Hydraulic Modelling of Civil Engineering Structures*, 1982, Coventry, U.K., pp. 22–24.
- [9] J. Yang, P. Teng, and H. Zhang, "Experiments and CFD modeling of high-velocity two-phase flows in a large chute aerator facility" *Journal of Engineering Applications of Computational Fluid Mechanics*, Vol 13(1), pp. 48-66, 2018.
- [10] H. Chanson, "Study of Air Entrainment and Aeration Devices" *Journal of Hyd. Research*, IAHR, Vol 27 (3), pp. 301-319, 1989a.
- [11] H. Chanson, "Aeration of a free jet above a spillway" *Journal of Hyd. Res., IAHR*, Vol 29(6), p. 864, 1991.
- [12] I. Schwartz, and L. P. Nutt, "Projected nappes subjected to transverse pressure" *Journal of the Hydraulics Division*, Vol 89(7), pp. 97–104, 1963.
- [13] S. b. Pan, , Y. y. Shao, Q. s. Shi, and X. l. Dong, "Selfaeration capacity of a water jet over an aeration ramp" *Shuili Xuebao Journal of Hydraulic Engineering*, Beijing, Vol 5, pp.13–22, 1980.
- [14] K. Kramer, and W. H. Hager, "Air transport in chute flows" *International Journal of Multiphase Flow*, Vol 31(10-11), pp. 1181–1197, 2005.
- [15] M. C. Aydin, and M. Ozturk, "Verification and validation of a computational fluid dynamics (CFD) model for air entrainment at spillway aerators" *Canadian Journal of Civil Engineering*, Vol 36(5), pp.826–836, 2010.
- [16] H. W. Zhang, Z. P. Liu, D. Zhang, and Y. H. Wu, "Numerical simulation of aerated high velocity flow downstream of an aerator." *Journal of Hydraulic Engineering*, Vol 39(12), pp. 1302–1308, 2008.
- [17] B. Ruidi, Z. Faxing, and L. Shanjun, "Air concentration and bubble characteristics downstream of a chute aerator" *International Journal of Multiphase Flow*, Vol 87, pp. 156–166, 2016.
- [18] P. Teng, J. Yang, and P. L. Ligier, "Air Demand Due to Flood Discharges at MOFORSEN dam – CFD Modelling with Field Measurements" E-proceedings of the 2nd International Symposium on Hydraulic Modelling and Measuring Technology, 2018, Nanjing, China, pp. 68–76.
- [19] J. Lian, C. Qi, F. Liu, W. Gou, S. Pan and Q. Ouyang, "Air Entrainment and Air Demand in the Spillway Tunnel at the Jinping-I Dam" *Journal of Applied Sciences*, Vol 7, pp. 89–112, 2017.
- [20] J. Yang, P. Teng, and C. Lin, "Air-vent layouts and water-air flow behaviors of a wide spillway aerator" *Journal of Theoretical & Applied Mechanics Letters*, Vol 9, pp. 130–143, 2019.
- [21] J. Yang, P. Teng, and Q. Xie, "Modelling of Air Demand of Spillway Aerators with Two-Phase Flow Model" E-proceedings of the 2nd International Symposium on Hydraulic Modelling and Measuring Technology, 2018, Nanjing, China, pp. 150–159.
- [22] P. Teng, J. Yang, and M. Pfister, "Studies of Two-Phase Flow at a Chute Aerator with Experiments and CFD Modelling" *Journal of Modelling and Simulation in Engineering* Vol 8, pp. 100–111, 2016.
- [23] B. Ruidi, S. Liu, Z. Tian, and Z. Faxing, "Experimental investigation of bubbly flow and air entrainment discharge downstream of chute aerators" *Journal of Environmental Fluid Mechanics*, Vol 19, pp. 1455–1468, 2019.
- [24] M. K. Sarvar, L. Ahmad, Z. A. Chaudary, and H. R. Mughal, "Experimental and numerical studies on orifice spillway aerator of Bunji Dam" *Journal of the Chinese institute of engineering*, Vol 6, pp. 68–79, 2019.
- [25] J. Yang, P. Teng, and H. Zhang, "Experiments and CFD modeling of high-velocity two-phase flows in a large chute aerator facility" *Journal of Engineering Applications of Computational Fluid Mechanics*, Vol 13(1), pp. 48–66, 2018.
- [26] M. C. Aydin, "Aeration efficiency of bottom-inlet aerators for spillways" *Journal of ISH Journal of Hydraulic Engineering*, Vol 7, pp. 124–136, 2017.
- [27] M. C. Aydin, E. Isik, and A. Emre Ulu "Numerical modeling of spillway aerators in high head dams" *Journal of ISH Journal of Applied Water Science*, Vol 10, pp. 178–188, 2020.
- [28] A. C. M. LIMA, "Caracterização da estrutura turbulenta em escoamentos aerados em canal de forte declividade com auxílio de técnicas de velocimetria a laser," Ph.D. dissertation, Escola de Engenharia, Universidade de São Paulo, São Carlos, Brasil, 2004.
- [29] OpenCFD Limited, "OpenFoam User Guide" 1.7.1 edition, 2016.
- [30] J. Tu, G. H. Yeoh, and C. Liu "Computational Fluid Dynamics" Springer, 3rd edition, 2019.